Exp Brain Res (2016) 234:241–254
DOI 10.1007/s00221-015-4449-8

RESEARCH ARTICLE

Single-cell coding of sensory, spatial and numerical magnitudes in primate prefrontal, premotor and cingulate motor cortices

Anne-Kathrin Eiselt[1,2] · **Andreas Nieder**[1]

Received: 20 March 2015 / Accepted: 18 September 2015 / Published online: 5 October 2015

Abstract The representation of magnitude information enables humans and animal species alike to successfully interact with the external environment. However, how various types of magnitudes are processed by single neurons to guide goal-directed behavior remains elusive. Here, we recorded single-cell activity from the dorsolateral prefrontal (PFC), dorsal premotor (PMd) and cingulate motor (CMA) cortices in monkeys discriminating discrete numerical (numerosity), continuous spatial (line length) and basic sensory (spatial frequency) stimuli. We found that almost exclusively PFC neurons represented the different magnitude types during sample presentation and working memory periods. The frequency of magnitude-selective cells in PMd and CMA did not exceed chance level. The proportion of PFC neurons selectively tuned to each of the three magnitude types were comparable. Magnitude coding was mainly dissociated at the single-neuron level, with individual neurons representing only one of the three tested magnitude types. Neuronal magnitude discriminability, coding strength and temporal evolution were comparable between magnitude types encoded by PFC neuron populations. Our data highlight the importance of PFC neurons in representing various magnitude categories. Such magnitude representations are based on largely distributed coding by single neurons that are anatomically intermingled within the same cortical area.

Keywords Single-neuron recording · Frontal cortex · Magnitude representation · Monkey

✉ Andreas Nieder
andreas.nieder@uni-tuebingen.de

Anne-Kathrin Eiselt
eiselta@janelia.hhmi.org

[1] Animal Physiology, Institute of Neurobiology, University of Tübingen, Auf der Morgenstelle 28, 72076 Tübingen, Germany

[2] Present Address: Janelia Research Campus, Howard Hughes Medical Institute, 19700 Helix Drive, Ashburn, VA 20147, USA

Introduction

In everyday life, we are confronted with different kinds of magnitudes, be it the number of dollar bills, the size of our coffee, or the brightness of our desk light. Judgments about numerosity magnitudes (like the number of dollar bills or dots in a display) are considered to be the most abstract form of quantity judgments (Diester and Nieder 2008; Nieder 2013; Nieder and Miller 2004; Nieder et al. 2002). Spatial, continuous magnitude dimensions (like size or line length) are more sensory-dependent given that sensory dimensions (such as spatial extent) are relevant. Still, spatial magnitudes also exhibit abstract properties because they require translation-invariant and generalized processing of sensory input (Tudusciuc and Nieder 2007; Vallentin and Nieder 2008). In contrast to numerosities, perceptual magnitudes (like light intensity or spatial frequencies, i.e., sinusoidal patches) constitute the most sensory magnitudes, because they are already neuronally represented at the level of the sensory epithelium and in early sensory processing areas (e.g., De Valois et al. 1982; Issa et al. 2000; Maffei and Fiorentini 1973; Peng and van Essen 2005; Robson et al. 1988).

Several psychophysical studies showed that different magnitude types influence one another perceptually, causing behavioral interference effects which support the notion of a (partly) overlapping neural representation of different magnitude dimensions (e.g., Dehaene and Changeux 1993; Walsh 2003). However, whether different magnitude types

share common neural resources or whether they are represented distinctly with similar coding properties remains unclear. Previously, Tudusciuc and Nieder (2007, 2009) compared the neuronal representation of numerosity and line length stimuli in a delayed match-to-sample task in non-human primates. They found that both magnitude types were encoded in the parietal and prefrontal cortex by distinct, but partly overlapping neuronal populations. A human functional imaging study by Pinel et al. (2004) reported differences in the degree of overlap of activated brain areas between sensory (like luminance/brightness) and spatial/numerical magnitude types: They each activated distinct, non-overlapping brain regions. These magnitudes (luminance on one hand, and spatial/numerical magnitude on the other hand) activated separate neural circuits and did not interact on the behavioral level. It was therefore suggested that brain areas involved in comparing perceptual dimensions like size and luminance differ from areas that integrate number and size at a more abstract representational level (Pinel et al. 2004).

So far, no electrophysiological study has investigated whether and how these three different magnitude types (like spatial frequency, size and number) are represented at the level of individual neurons. It is therefore unknown whether single neurons can encode several magnitude types simultaneously or rather are dedicated to a specific magnitude only. Moreover, the respective contribution of frontal lobe areas in the coding of different magnitude types remains elusive.

To address these questions, we compare the neuronal representation of three different magnitude types in three simultaneously recorded frontal areas (prefrontal, dorsal premotor and cingulate motor cortex) of behaviorally trained monkeys. We previously reported rule-related activity in 'greater than'/'less than' decisions based on numerosity and line length stimuli (Eiselt and Nieder 2013, 2014). In the current study, we focus exclusively on (a) the initial encoding and memorization phase, before any rule information was conveyed in the trial, and (b) introduce a third, purely sensory magnitude, namely spatial frequency (i.e., 'gabor patch').

Materials and methods

Subjects

We collected data from two male macaque monkeys (*Macaca mulatta*, monkey O: 8 kg; monkey E: 4 kg) that were trained first on the numerosity comparison, followed by the line length and finally the spatial frequency comparisons. All training, surgeries and experimental procedures were performed in accordance with the guidelines for animal experimentation approved by the Regierungspraesidium Tuebingen, Germany.

Behavioral task

Monkeys were trained on a 'greater than' and 'less than' comparison task and judged whether a test quantity was smaller/shorter/lower or larger/longer/higher than a sample quantity. In each session, they had to flexibly apply these rules to three different magnitude types (or categories): the spatial frequency of a sine-wave grating (visuo-sensory magnitude), the length of a line (visuo-spatial magnitude) and the number of dots in a set (visuo-numerical magnitude). Monkeys initiated a trial by grabbing a response bar and fixating a central fixation target (Fig. 1a). Eye movements were monitored with an infrared eye-tracking system (ISCAN, Burlington, MA, USA), and fixation was required to stay within a window of 1.75° around the fixation target until the response phase (test1 phase). After 500 ms of initial fixation, a sample stimulus was presented for 500 ms and displayed the reference magnitude value. The sample presentation was then followed by a memory period of 1000 ms (delay1). Next, a rule cue (500-ms duration) indicated whether the monkey had to apply the 'greater than' rule or the 'less than' rule, which was again followed by a 1000-ms delay (delay2). In the response phase, monkeys were required to release the response bar if the presented test1 magnitude value (presented for 1200 ms) was larger/longer/higher (smaller/shorter/lower) than the sample value and the 'greater than' ('less than') rule had been cued. However, if the 'less than' ('greater than') rule had been cued and the test1 magnitude was larger/longer/higher (smaller/shorter/lower) than the sample magnitude, respectively, monkeys had to keep holding the response bar throughout the test1 phase and wait for the test2 magnitude (which was always the correct response stimulus). In 50 % of the trials (match trials), the magnitude value in the test1 period matched the cued rule; in the other half of the trials (non-match trials), the magnitude value did not match the cued rule and, hence, the monkey needed to withhold the release of the response bar until the second test display (test2) was presented. Each rule was signified in two different sensory modalities: a red circle or a white circle delivered with a drop of water indicated the 'larger/longer/higher than' rule, whereas a blue circle or a white circle delivered with no water cued the 'smaller/shorter/lower than' rule. The amount of water delivered to indicate the 'larger/longer/higher than' rule was a very small drop and thus not suited as a reward. It exclusively served as a second, i.e., non-visual, modality to indicate the rule. For more details concerning the task see Eiselt and Nieder (2013). All relevant features (e.g., sensory, spatial and numerical magnitude, sample magnitude values, 'greater than' and 'less than' rule, rule cue modality) were randomized and balanced across trials.

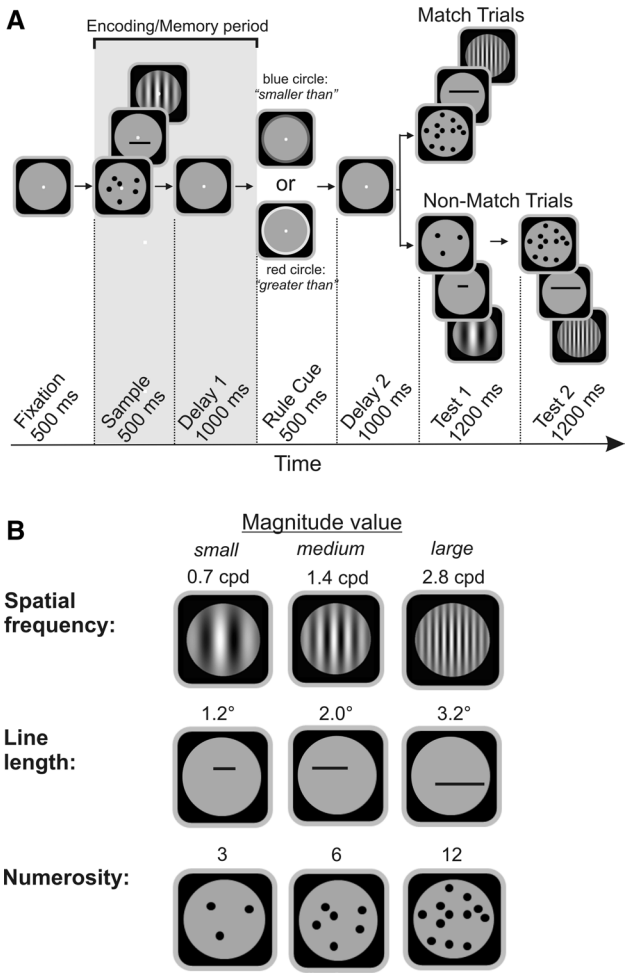

Fig. 1 Behavioral protocol and stimuli. **a** After grabbing a response *bar* and maintaining fixation, a sample spatial frequency, line length or numerosity quantity was presented followed by delay1 phase. Next, a rule cue instructed the monkey to apply the appropriate rule ('greater than' or 'less than'), followed by a second delay (delay2). In the response phase, a corresponding test magnitude of the same magnitude type was presented and monkeys had to release the *bar* if the test magnitude was in agreement with the cued rule. In non-match trials, where the test1 magnitude did not correspond with the cued rule, monkeys had to withhold their response until the test2 phase when the corresponding test magnitude was presented. Only neuronal responses to the sample and the delay1 period (*gray area*) are analyzed in the current study. **b** Example quantity stimuli for spatial frequency (sensory magnitude), line length (spatial magnitude) and numerosity (numerical magnitude) are shown. Each magnitude was presented in three different (small, medium and large) values

Stimuli

We used three different visual magnitude (or quantity) types (Fig. 1b): the spatial frequency of visual sine-wave gratings, length of lines and the number of items in a set (numerosities). Magnitudes were displayed in black (lines and numerosities) and black/white (sine-wave gratings, 100 % modulation depth) on a gray background (diameter: 7° of visual angle). We used three different magnitude values (small, medium and large) for each magnitude type. Spatial frequency stimuli consisted of sample spatial frequencies of 0.7 cycles per degree (cpd) (lower test spatial frequency = 0.35 cpd, higher test spatial frequency = 1.4 cpd), 1.4 cpd (0.7, 2.8 cpd) and 2.8 cpd (1.4, 5.6 cpd). Sine-wave gratings were convolved with a gaussian 2D kernel to prevent sharp edges of the aperture (i.e., a 'gabor patch'). Line length stimuli included line lengths of 1.2° of visual angle (shorter test line length = 0.75°, longer test line length = 2°), 2° (1.2°, 3.2°) and 3.2° (2°, 5°), with line thicknesses ranging from 0.06° to 0.36°. For the numerosity stimuli, we presented sample numerosities 3 (smaller test numerosity = 1, larger test numerosity = 6), 6 (3, 12) and 12 (6, 24). For each session, all stimuli were generated anew using MATLAB (MathWorks, Natick, MA, USA). The phase of the sine-wave gratings, the position and thickness of the lines, and the size and position of the numerosity dots (diameter range 0.3°–1.3°) varied randomly.

To exclude that the animals used non-quantity-related information to perform the task by attending to low-level visual features, we additionally presented control magnitude stimuli in which visual parameters were equated between the sample and the respective match and non-match images. In each session, control stimuli were randomly intermixed and presented with the same frequency as the standard stimuli. For numerosity control stimuli, dot density and total pixel area (i.e., contrast) across numerosities were controlled. Line length control stimuli were equated for total pixel area, and control stimuli for sine-wave gratings were rotated by 90°. Overall, 144 specific trial conditions were tested in every session: 3 magnitude types (spatial frequency, line length and numerosity), 3 magnitude sample values (e.g., 3, 6 and 12 dots for numerosity), 2 stimulus protocols (standard and control), 2 rules (greater than and less than), 2 rule cues (color blue/red and with/without drops of water) and 2 trial types (match and non-match).

Before electrophysiological recording, generalization trials were introduced to test whether the monkeys could generalize the task to novel stimuli. In these trials, monkeys had to respond to new sample stimuli for each magnitude type that had not been used during training and thus were completely unknown to the animals. Generalization trials included the spatial frequency 1.1 cpd (lower test spatial frequency = 0.54 cpd, higher test spatial frequency = 2.14 cpd), the line length 1.3° (shorter test line length = 0.813°, longer test line length = 2.08°) and the numerosity 4 (smaller test numerosity = 2, larger test numerosity = 8). Behavioral performance to generalization trials is shown in Fig. 2.

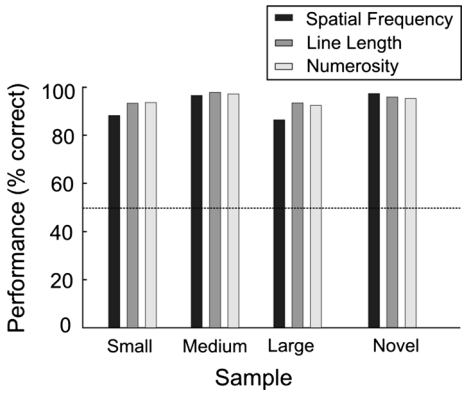

Fig. 2 Average behavioral performance of both monkeys. Percent of correct responses for the smallest, medium and largest sample and generalization (new) stimuli in either spatial frequency, line length or numerosity trials during recording sessions. Performance is averaged across monkeys, rules, rule cues and protocols. *Dark gray bars* correspond to spatial frequency, *medium gray* to line length, and *light gray* to numerosity trials. Chance level is 50 %

Electrophysiological recordings

Extracellular single-cell activity was recorded from three areas simultaneously: the right prefrontal (PFC) (centered above the principal sulcus (PS), Brodmann area 46), the left dorsal premotor cortex (PMd) and in the left cingulate sulcus from parts of the dorsal cingulate motor area (CMAd) and rostral cingulate motor area (CMAr). CMA recordings were made below the PMd recording location at 7.5–10.5 mm depths. No signals were detected at depths ranging from 5 to 7 mm below the cortical surface, indicating that our recording sites were lateral to the medial wall. The positions of the recording chambers were calculated using stereotaxic coordinates and were reconstructed using MRI images of both monkeys (Eiselt and Nieder 2014). Arrays of eight glass-coated tungsten microelectrodes of 1-MΩ impedance (Alpha Omega) were used and lowered into the brain through a grid with 1 mm spacing using custom-made microdrives. Recorded spikes were amplified, filtered, digitized and stored using a Multichannel Acquisition Processor (Plexon); spike sorting was performed offline (Off Line Sorter, Plexon). Neurons were recorded randomly; there was no attempt to preselect cells according to task-related activity.

Data analysis

For all analysis and statistical tests, MATLAB (MathWorks, Natick, MA, USA) was used. Behavioral performance was individually computed for each condition. Neuronal sample activity was derived from a 500-ms interval after stimulus onset shifted by 100 ms. Delay1 (see Fig. 1a) activity was calculated over an 800-ms window after sample offset, shifted by 200 ms. A two-way ANOVA with a conservative P value of $P < 0.01$ (to account for threefold testing of a cell in the sample task period) was computed separately for the numerosity, line length and spatial frequency protocol for each neuron, with factors quantity (e.g., spatial frequencies of 0.7, 1.4 and 2.8 cpd) and stimulus type (standard or control) for either the sample or delay1 period.

For each sample-selective neuron during the sample or delay1 period, we computed a selectivity-strength (SST) and selectivity-sharpness (SSH) index (Vallentin and Nieder 2010). The SST was calculated by subtracting the minimum firing rate of the neuron (the response to the least preferred sample stimulus) from the maximum firing rate of that neuron (firing rate in response to the preferred sample stimulus) divided by the sum of both. Thus, values of SST close to 1 indicate high selectivity. We also calculated a selectivity-sharpness index (SSH) by subtracting the median firing rate of all three sample stimuli from the firing rate to the preferred sample stimulus. i.e., the index is the difference between the firing rate to the most preferred stimulus and the median firing rate to all three sample stimuli. This quantifies the width of the selectivity curve and high values correspond to sharper tuning for the preferred stimulus in relation to the other two sample stimuli.

Using receiver-operating-characteristic (ROC) analysis (Green and Swets 1966), we calculated the mean area under the ROC curve (AUROC) value between the preferred and non-preferred sample in a fixed time window for the sample (500-ms duration, 100-ms offset) and delay1 (800-ms duration, 200-ms offset) period. The ROC value corresponds to the probability that an observer could identify the current sample solely based on the neural firing rate of a single neuron. ROC values of 1 would indicate a perfect discrimination between the preferred and non-preferred sample, whereas a values of 0.5 indicate no differentiation between the two samples. We computed the mean AUROC values between the preferred and non-preferred samples for each magnitude protocol separately for neurons with sample selectivity in the sample and delay1 period. Each selective neuron was tested individually using the responses to the preferred and least preferred sample stimulus, and thus, AUROC values indicate how well a given neuron encodes the sample. To compare the strength and temporal evolution of the coding quality of sample-selective neurons, we also calculated a sliding-window ROC analysis using a 100-ms window slid in 5-ms steps throughout the entire trial.

To further characterize the time points at which each neuron significantly encoded the sample, we computed a second sliding-window ROC analysis between fixation onset and the delay1 offset in 20-ms steps (window size 100 ms) in combination with a permutation test. In each time window, we computed a null distribution by shuffling the firing rate distributions of the preferred and least

preferred sample stimulus and randomly assigned them again to either category (preferred vs. least preferred). If the obtained (real) AUROC value exceeded the upper 95 % threshold of the null distribution of AUROC values in four consecutive time windows, the first significant analysis window was then taken as the neuron's latency for sample selectivity. In addition to the latency measure of sample selectivity based on the ROC analysis, we performed a sliding Kruskal–Wallis test (50-ms window, step size 5 ms) for each magnitude protocol as a second test for magnitude-selectivity latency and to verify the AUROC latency results.

Besides determining the latency of selectivity to the magnitudes, we also calculated the plain visual response latencies for neurons responding to either spatial frequency, line length, or numerosity. For visual response latency, we compared the firing rate of a 10-ms window, slid by 5 ms, with the mean firing rate during the first 350 ms of the fixation period (baseline firing rate). The time point at which the firing rate exceeded three standard deviations (SD) above the baseline determined the neurons ('visual') response latency, which served as the third comparison of latency differences between neurons responding to different magnitude categories.

Results

Behavioral performance

Two monkeys performed a rule-guided magnitude discrimination task (Fig. 1a). The task required the monkeys to perceive and memorize three different types of sample magnitudes: the spatial frequency of a sine-wave grating as a basic visuo-sensory magnitude, the length of a line representing a continuous visuo-spatial magnitude or the number of items in dot displays (numerosity) as a discrete visuo-numerical magnitude. Three different sample values (small, medium and large) were presented for each magnitude type (Fig. 1b).

For both monkeys, the overall performance to the three different magnitude types (spatial frequency, line length and numerosity) was comparable ($P > 0.05$, Mann–Whitney U test) and significantly above chance level ($P < 0.001$, binomial test) (see Fig. 2). For a more detailed behavioral analysis regarding quantitative rules see Eiselt and Nieder (2013). Generalization trials, in which new sample values for each magnitude type were presented, ensured that the monkeys solved the task based on a general grasp of quantity, irrespective of the absolute sample value. Both monkeys correctly solved on average 96 % of the generalization trials ($P < 0.001$, compared with chance expectation) which is comparable to the well-trained baseline trials (Fig. 2).

General neuronal response properties

In the present study, we focused on the question of how neurons in the frontal lobe actively encode sensory representations of different types of magnitudes and maintain this information in working memory during a delay period. We therefore recorded neural activity during a rule-based magnitude discrimination task and analyzed the sample and the first memory delay (delay1) period (Fig. 1a) from three separate areas of the frontal lobe. Overall, we analyzed the activity of 395 single units from the lateral prefrontal cortex (PFC), 349 single units from the dorsal premotor cortex (PMd) and 204 single units from the depth of the cingulate motor cortex (CMA), resulting in a total of 948 recorded and analyzed neurons.

First, we determined sample-selective cells in each brain area using a two-way ANOVA ($P < 0.01$), with magnitude value (smallest, medium or largest) and stimulus protocol (standard or control) as main factors, for either the sample or delay1 period separately for each magnitude type. Only neurons showing exclusively a main effect of spatial frequency, line length or number were regarded as magnitude-selective neurons. The numbers and proportions of selective neurons are listed in Table 1. Figure 3 shows the recorded brain areas (Fig. 3a), as well as precise anatomical locations and percentages of sample-selective neurons for each magnitude type in monkey E (*left panel*) and monkey O (*right panel*) in the PFC (Fig. 3b), the PMd (Fig. 3c) and the CMA (Fig. 3d). Neurons in CMA of monkey O were recorded either anterior (CMAr) or posterior (CMAd) to the genu of the arcuate sulcus (dashed line in Fig. 3d, *right panel*), whereas only CMAr neurons were recorded from monkey E (see also Eiselt and Nieder 2014). Since no sample-selective neurons were found in CMAr and CMAd of monkey O, CMA is equivalent to CMAr in the current study.

Overall, 26 % of all recorded neurons in PFC (101/395) showed a significant magnitude value effect for either magnitude type during the sample (19 %, 75/395) and/or delay1 period (10 %, 41/395). Almost 15 % of these cells were active during both trial periods (15/101), but did not necessarily prefer the same magnitude type in both trials periods ($P > 0.05$, binomial test). In PMd, only 5 % (17/349) of all recorded neurons were magnitude value-selective in the sample (2 %, 6/349) and/or delay1 period (4 %, 13/349), with only one neuron being active in both trial periods. In CMA, hardly any (3 %, 6/204) of the recorded cells showed sample selectivity during the sample (2 %, 4/204) or delay1 (1 %, 2/204) period, which corresponds to chance expectation. Figure 4a, b depicts the percentages of magnitude value-selective cells of all recorded neurons separately for each magnitude type in the three recorded brain areas for the sample (Fig. 4a) or delay1 period (Fig. 4b). In both trial

Table 1 Distribution of neurons selective to the sample or protocol during either the sample or delay1 period in each recorded area

	Spatial frequency	Line length	Number
PFC (n = 395)			
Sample period Sample	28 (7 %)	36 (9 %)	21 (5 %)
Protocol	21 (5 %)	0 (0 %)	12 (3 %)
Sample × protocol	6 (2 %)	2 (1 %)	7 (2 %)
Delay1 period			
Sample	14 (4 %)	14 (4 %)	16 (4 %)
Protocol	17 (4 %)	3 (1 %)	10 (3 %)
Sample × protocol	3 (1 %)	0 (0 %)	1 (0 %)
PMd (n = 349)			
Sample period			
Sample	2 (1 %)	1 (0 %)	3 (1 %)
Protocol	6 (2 %)	3 (1 %)	11 (3 %)
Sample × protocol	0 (0 %)	0 (0 %)	1 (0 %)
Delay1 period			
Sample	5 (1 %)	5 (1 %)	3 (1 %)
Protocol	0 (0 %)	2 (1 %)	8 (2 %)
Sample × protocol	0 (0 %)	0 (0 %)	0 (0 %)
CMA (n = 204)			
Sample period			
Sample	2 (1 %)	1 (1 %)	1 (1 %)
Protocol	1 (1 %)	3 (2 %)	2 (1 %)
Sample × protocol	0 (0 %)	1 (1 %)	0 (0 %)
Delay1 period			
Sample	1 (1 %)	0 (0 %)	1 (1 %)
Protocol	2 (1 %)	2 (1 %)	1 (1 %)
Sample × protocol	0 (0 %)	0 (0 %)	0 (0 %)

Selectivity was defined using a two-way ANOVA ($P < 0.01$, see "Materials and methods") during two trial periods. Proportions are based on all recorded neurons in each area

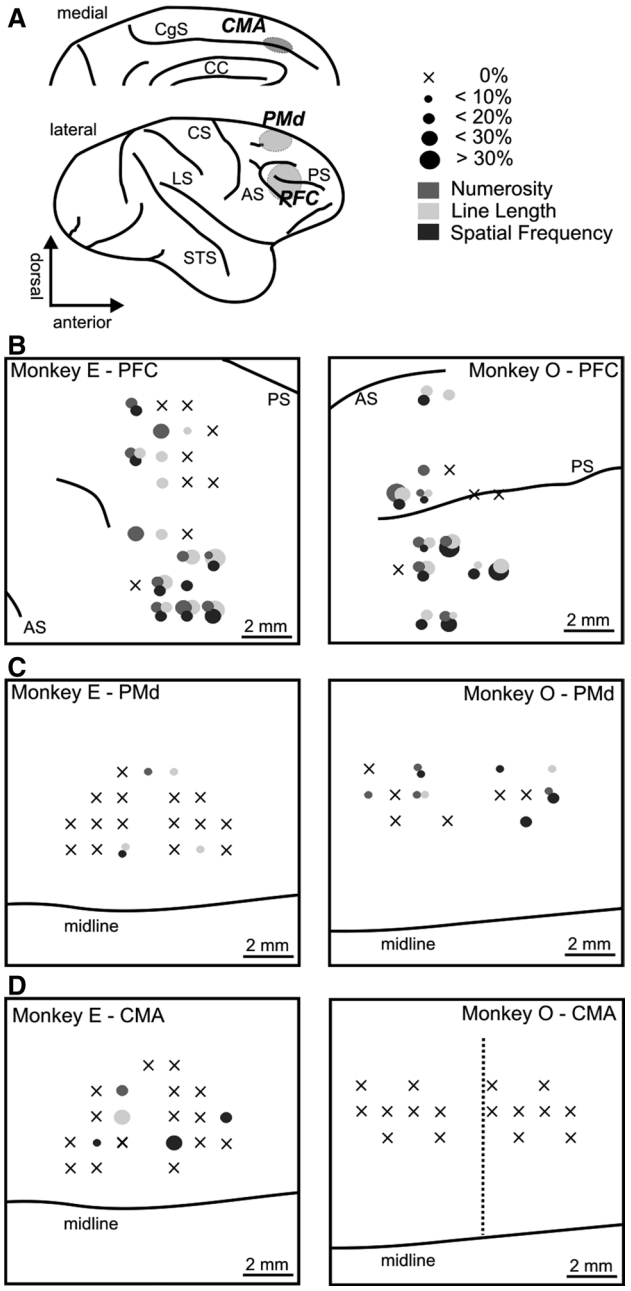

Fig. 3 Recording locations in the PFC, PMd and CMA. **a** General recording areas on a lateral and medial view of a monkey brain. **b** Recording sites and location of sample-selective cells (*color-coded*) for monkey E and monkey O in PFC, **c** PMd and **d** CMA. *AS* arcuate sulcus, *CC* corpus callosum, *CgS* cingulate sulcus, *CS* central sulcus, *LS* lateral sulcus, *PS* principal sulcus, *STS* superior temporal sulcus

periods (sample and delay1), we found significantly more magnitude value-selective cells in PFC compared to PMd and CMA ($P < 0.01$, Chi-square test). There was no significant difference in the proportion of magnitude value-selective cells between PMd and CMA ($P > 0.05$, Chi-square test). Because the frequencies of sample-selective cells in PMd and CMA were close to chance expectation, these two brain areas are not further discussed. Thus, all following results are based on the population of PFC neurons only.

Proportions of magnitude-selective cells in PFC

The activity of three example PFC neurons selectively tuned to the value of only one magnitude type in the sample period is shown in Fig. 5. The neuron in Fig. 5a was only selective for spatial frequency stimuli, preferring the large sample value (spatial frequency of 2.8 cpd), and did not differentiate between the magnitude values of the line length and numerosity stimuli. A second example neuron (Fig. 5b) was only tuned to line length stimuli (preferred line length of 2° visual angle, the medium value) and indifferent for spatial frequency and numerosity stimuli. Finally, a third example neuron (Fig. 5c) exhibited numerosity selectivity (preferring the largest numerosity 12), but no length or spatial frequency selectivity.

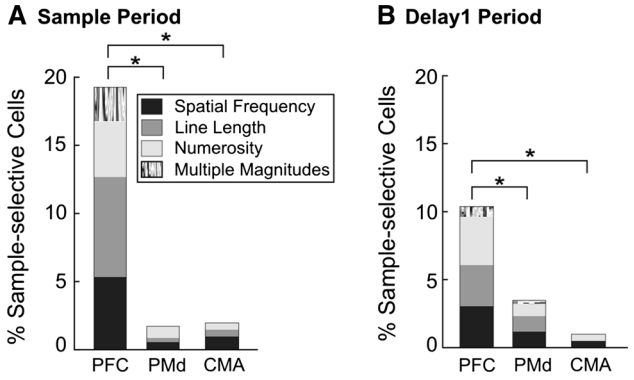

Fig. 4 Proportion of sample-selective cells. Percent sample-selective cells in PFC, PMd and CMA for each magnitude type in **a** the sample and **b** delay1 period. *Asterisks* indicate $P < 0.01$

Of all magnitude-selective PFC neurons tuned during sample presentation, 37 % (28/75) were tuned to spatial frequencies, 48 % (36/75) to line length and 28 % (21/75) to numerosity. As can be seen in the Venn diagram in Fig. 5d, 10 of these 75 (13 %) magnitude-selective PFC cells showed significant tuning to more than a single magnitude type (e.g., for spatial frequency and line length). However, the number of cells exhibiting selectivity for multiple magnitude types was indifferent from chance expectation, i.e., the overlap between the populations of selective sample neurons tuned to different magnitudes was expected by chance ($P > 0.05$, binomial test, separately tested for each population overlap).

In the memory (delay1) period, 34 % (14/41) of the magnitude-selective PFC cells encoded spatial frequency, 34 % (14/41) represented line length and 39 % (16/41) numerosity stimuli (Fig. 5e). Of all delay1-magnitude-selective PFC cells, 7 % (3/41) were tuned to two magnitude types, which was equal to chance prediction ($P > 0.05$, binomial test), i.e., the overlap between the populations of selective neurons tuned to multiple, different magnitudes was again indifferent from chance expectation.

Strength and sharpness of sample selectivity in PFC

To further analyze possible sample coding differences between the three magnitude types, we first calculated the selectivity-strength index (SST) for each neuron individually (see "Data analysis"). The strength of selectivity indicates how well a neuron discriminates between its preferred and least preferred stimulus. The results are shown in Fig. 6a separately for the sample and delay1 period. The selectivity-strength index (SST) was not significantly different between the three magnitude types (spatial frequency: SST = 0.41 and 0.34 for the sample and delay1 period, respectively; line length: SST = 0.53 and 0.37; numerosity: SST = 0.39 and 0.52; $P > 0.05$, Mann–Whitney U test). This suggests that the sensitivity and strength of magnitude coding in PFC is similar for visuo-sensory, visuo-spatial and visuo-numerical magnitudes. To compare the average SST values between sample and delay1 periods, we pooled those values across magnitude types and found no significant differences in discrimination between the preferred and least preferred stimulus in the sample and delay1 phase of the trial ($P > 0.05$, Mann–Whitney U test).

Next, we quantified the width of the magnitude tuning curves and calculated the selectivity-sharpness index (SSH) for each neuron (see "Data analysis"). Figure 6b shows the average SSH for the sample and delay1 period separately for the three magnitude types. The SSH values between spatial frequency (SSH = 3.14 and 2.53, for sample and delay, respectively), line length (SSH = 4.62 and 2.35) and numerosity (SSH = 4.6 and 2.93) stimuli were not significantly different ($P > 0.05$, Mann–Whitney U test). This indicates that the neurons of these three populations (selectively tuned to either spatial frequency, line length or numerosity) were tuned equally sharp to their preferred sample value. Thus, we pooled the SSH values across magnitude types to compare the average SSH values between sample and delay1 periods, and we found that the sharpness indices in the sample and delay1 phase had similar values ($P > 0.05$, Mann–Whitney U test).

Temporal evolution and quality of magnitude coding in PFC

To quantify the quality of magnitude selectivity in PFC neurons, we applied a ROC analysis to the neuronal activity in the same time windows as used for the ANOVA. Magnitude selectivity in the sample phase was measured in a 500-ms window (starting 100 ms after sample onset), whereas in the delay1 period an 800-ms window (starting 200 ms after sample offset) was used. The values of the area under the ROC curve (AUROC) could range from 0.5 (no discriminability between most and least preferred magnitude value) to 1.0 (perfect discriminability). As shown in Fig. 7a, the AUROC values were comparable for spatial frequency (mean AUROC = 0.76 and 0.77 for the sample and delay1 period, respectively), line length (mean AUROC = 0.77 and 0.72) and numerosity (mean AUROC = 0.76 and 0.73) (Mann–Whitney U test $P > 0.05$). Also the magnitude-pooled AUROC values in the sample and delay1 phase were similar ($P > 0.05$, Mann–Whitney U test).

To investigate the temporal evolution of magnitude selectivity in the PFC, we computed a sliding-window ROC analysis throughout the whole trial (100-ms window slid in 5-ms steps) for each magnitude type separately. The pooled values of all selective neurons are shown in Fig. 7b for the sample phase, and in Fig. 7c for the delay1 period. From

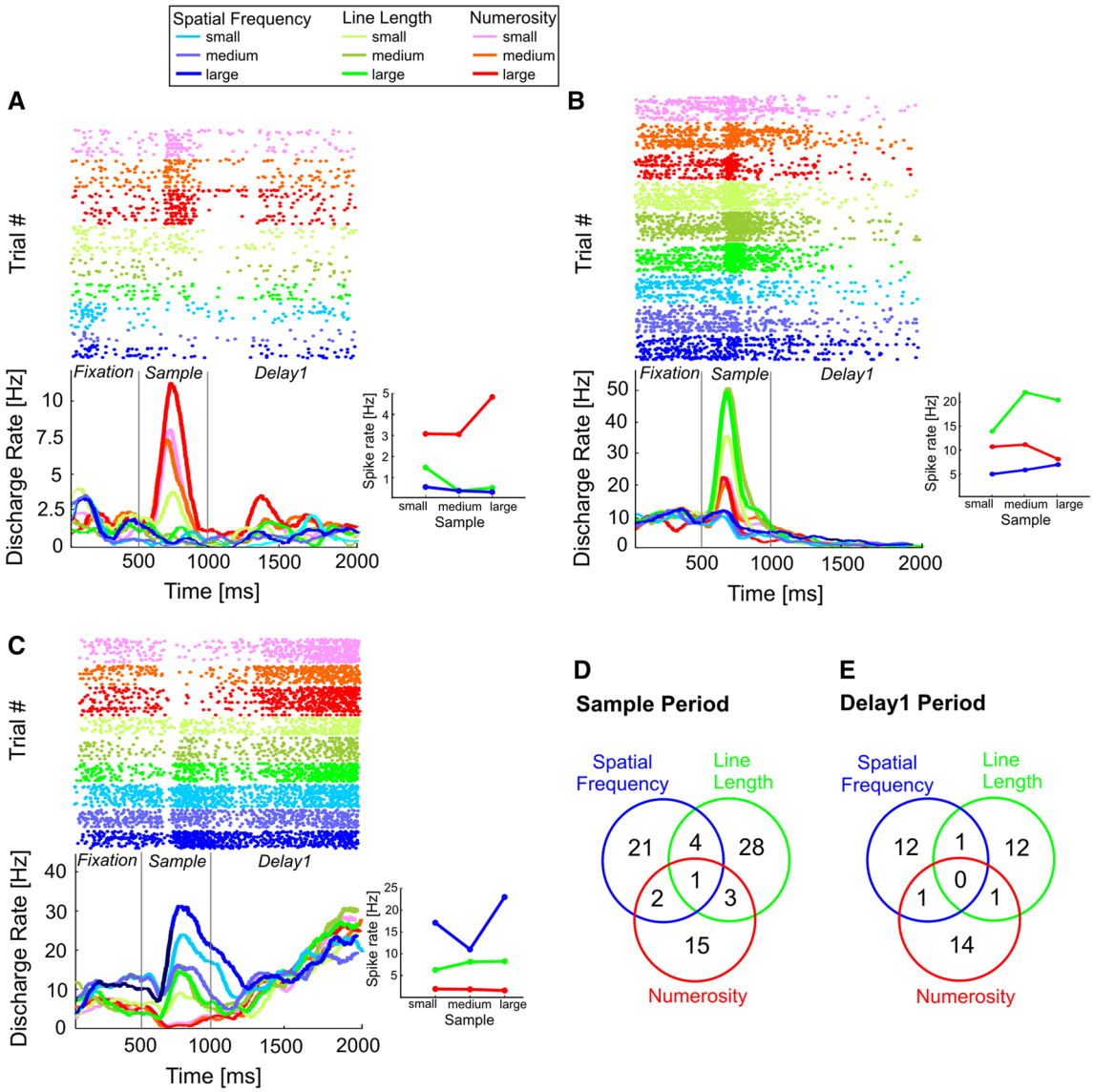

Fig. 5 Three magnitude-selective example neurons and the proportion of magnitude selectivities in the PFC **a**–**c** PFC example neurons exhibiting sample selectivity during the sample period. **a** Example neuron tuned to highest numerosity (numerosity 12), but not to spatial frequency or line length stimuli. Dot-raster histogram (each *dot* represents an action potential, spike trains are sorted and color-coded according to the magnitude type and sample) is plotted above the spike-density averages (averaged over all trials and smoothed by a 150-ms Gaussian kernel). **b** Neuron tuned to medium line length, but without sample selectivity to spatial frequency or numerosity stimuli. **c** Neuron tuned to spatial frequency (preferring the highest spatial frequency), but not to line length or numerosity. Inlets represent the tuning functions of the respective neurons for spatial frequencies, line lengths and numerosities during the sample period. **d**, **e** Venn diagrams depict the number of PFC neurons selectively encoding spatial frequency, line length and/or numerosity sample stimuli during the **d** sample and **e** delay1 period

this data, we determined the time points at which individual magnitude-selective neurons started to show significant magnitude coding during the sample phase.

Figure 8 shows individual neurons' sliding AUROC values throughout the fixation, sample and delay1 period for neurons tuned to spatial frequency (Fig. 8a), line length (Fig. 8b) and numerosity samples (Fig. 8c). The neurons are sorted according to the first of four consecutive time windows in which that neuron significantly differentiated between the samples for each magnitude type ($P < 0.05$, permutation test; see "Data analysis" for details) and, thus, depicts the latency of each neuron in the sample period. The mean latencies for spatial frequency (222 ms), line length (247 ms) and numerosity trials (238 ms) were indifferent ($P > 0.05$, Kruskal–Wallis test). An additional latency analysis (sliding Kruskal–Wallis test, 50-ms window, step size 5 ms) for each magnitude type separately confirmed that the three different magnitude dimensions were encoded

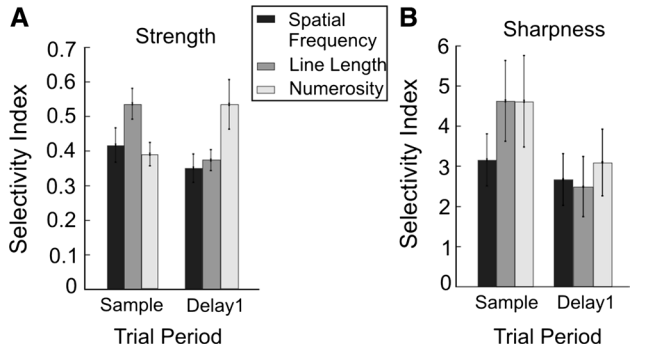

Fig. 6 Selectivity strength and sharpness of PFC neurons. **a** Mean selectivity strength of neurons tuned to spatial frequency, line length or numerosity stimuli during the sample and delay1 period. **b** Mean selectivity sharpness for the three magnitudes and both trial periods. *Error bars* represent standard error

equally fast ($P > 0.05$, Kruskal–Wallis test). Finally, we compared the general ('visual') response latencies (see "Data analysis") between neurons responding to spatial frequency (mean RT = 150 ms), line length (190 ms) or numerosity (175 ms) stimuli and found no significant difference between them ($P > 0.05$, Mann–Whitney U test). This suggests that sensory, spatial and discrete quantities are represented (or processed) with a comparable speed within prefrontal cortex.

Discussion

In the current study, we compared the neuronal representation of three different magnitude types (visuo-sensory, visuo-spatial and visuo-numerical magnitudes) in three

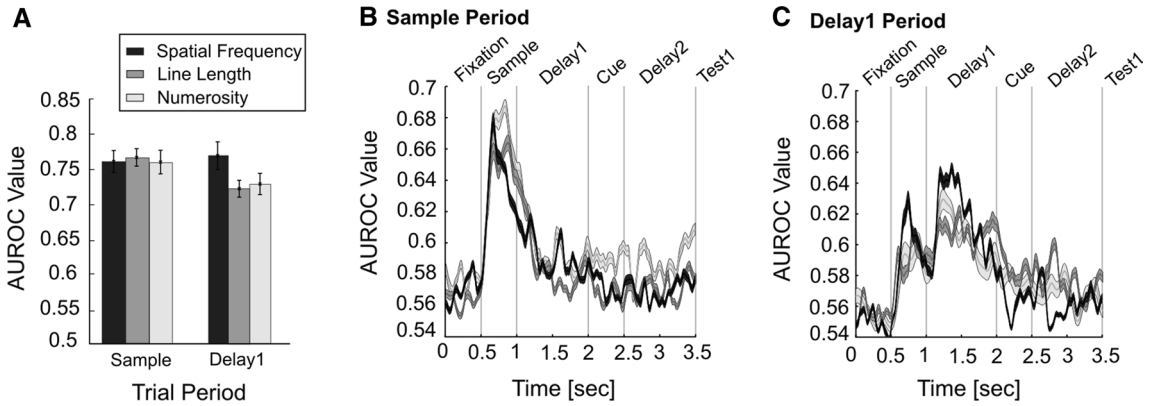

Fig. 7 Average AUROC values of PFC neurons for the three different magnitude types. **a** Mean AUROC value in a static window for sample-selective PFC cells tuned to spatial frequency, line length or numerosity stimuli either in the sample (500-ms window, starting 100 ms after sample onset) or in delay1 (800-ms window, starting 200 ms after sample offset) period. **b**, **c** Mean AUROC value for spatial frequency (*dark gray*), line length (*medium gray*) and numerosity (*light gray*) trials computed in a sliding-window ROC analysis (100-ms window, 5-ms step size) throughout the whole trial (smoothed by a 5-ms Gaussian kernel) for PFC neurons showing sample selectivity in the **b** sample or **c** delay1 period

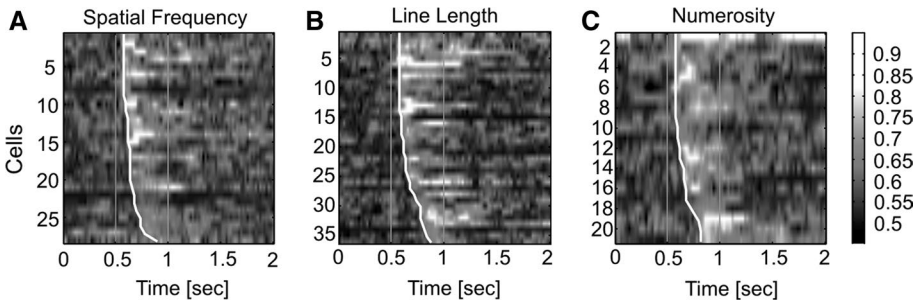

Fig. 8 Timing of sample selectivity of PFC neurons during the sample phase tuned to **a** spatial frequency, **b** line length and **c** numerosity stimuli. Each row corresponds to one individual neuron. Strength of sample selectivity (AUROC value) is color-coded, and neurons are sorted according to their selectivity latency (*white line*). Temporal evolution of sample-selective signals is plotted from start of fixation (time 0 s) until the end of delay1 (at 2 s). *Gray lines* correspond to the duration of sample presentation (onset and offset)

different areas of the frontal lobe in a rule-guided magnitude comparison task. We asked whether areas typically associated with simple stimulus–response association activity (PMd) or monitoring (CMA) also represent the underlying quantity information in a rule-guided magnitude comparison task. Alternatively, the lateral prefrontal cortex (PFC), which is known for its involvement in quantity processing (e.g., Genovesio et al. 2005, 2009, 2011; Hayashi et al. 2013; Nieder 2013; Nieder and Miller 2004; Onoe et al. 2001; Piazza et al. 2007; Rao et al. 2001; Tudusciuc and Nieder 2009), might be a special key area in integrating quantitative information. The combined results from the current and a previous study (Eiselt and Nieder 2014) suggest a privileged position of the PFC in encoding magnitude and rule information in a rule-guided magnitude discrimination task. In the current study, we find that neurons in PMd and CMA are not (more than expected by chance) encoding magnitudes during the sample and delay periods. In addition, only a very small portion (6 %) of cells in CMA and PMd encoded the rule (Eiselt and Nieder 2014). This is in contrast to 24 % of rule-selective cells (Eiselt and Nieder 2014) and 25 % of sample-selective cells (current study) in the PFC. In the current study, we found that 25 % of all recorded neurons in PFC exhibited sample selectivity for either spatial frequency, line length or numerosity stimuli, with a similar number of neurons representing each of the three different magnitude types. An overlap of PFC neurons encoding spatial frequency, line length or numerosity beyond chance expectation was not observed. The discriminability, coding strength and temporal evolution of representational signals was comparable for the three classes of magnitudes, suggesting similar coding properties for the different magnitude types in PFC. Overall, this indicates that the PFC might not only be particularly important for guiding rule-based decisions, but also for integrating different magnitude information.

Representation of sensory magnitudes in PFC

In the current study, we found that PFC neurons represent sensory magnitudes, like the frequency of a sine-wave grating, similar to more abstract magnitude types. The coding properties (selectivity-strength, selectivity and sharpness index, temporal properties) for the sensory spatial frequency representation were comparable to more abstract magnitudes like continuous spatial and discrete numerical magnitudes.

We used spatial frequency stimuli as the sensory magnitude, since it is a controllable stimulus that yielded similar discrimination performance compared to more abstract line length and numerosity stimuli discriminations. Pilot training on intensity stimuli, in which monkeys had to judge the intensity of a presented stimulus, did not result in a comparable discrimination performance (unpublished data) and were therefore not used in the present study. Since spatial frequencies, unlike line lengths and numerosities, are already represented in early visual processing areas (De Vois et al. 1982; Issa et al. 2000; Robson et al. 1988), we classified them as a sensory magnitude.

The PFC is usually implicated in the active maintenance and processing of task relevant information. However, PFC neurons have been shown several times to represent visual information reminiscent of extrastriate visual cortex. Hussar and Pasternak (Hussar and Pasternak 2009, 2012, 2013), for example, found that purely sensory magnitudes, like the speed and direction of moving random-dot stimuli, are represented in PFC. The tuning properties of visual motion-selective PFC neurons mirror those observed in the motion processing middle temporal (MT) cortical area. Additionally, they observed that the majority of task-sensitive neurons were selective for both speed and motion direction, and suggested a generalized neural mechanism for the comparison of sensory signals in PFC (Hussar and Pasternak 2013). Sensory attributes of mnemonic representations were also reported by Constantinidis et al. (Constantinidis et al. 2001) who found that PFC activity reflected graded variations in the luminance of a to-be-remembered stimulus. In the somatosensory domain, Romo et al. (1999) observed a parametric representation of the frequency of a remembered vibratory stimulus. Collectively, this indicates that sample and memory activity in PFC represents perceived sensory attributes of stimuli, in addition to abstract rule and decision signals (e.g., Assad et al. 2000; Bongard and Nieder 2010; Eiselt and Nieder 2013; Genovesio et al. 2005; Hoshi et al. 1998; Merten and Nieder 2012, 2013; Wallis and Miller 2003; Wallis et al. 2001; White and Wise 1999).

Neuronal populations and magnitude representations

Behavioral interference effects in psychophysical tasks (de Hevia et al. 2008; Dormal and Pesenti 2007, 2009; Henik and Tzelgov 1982; Lu et al. 2009; Schwarz and Eiselt 2009; Xuan et al. 2007) and functionally overlapping brain regions activated by different magnitude information (e.g., Dehaene et al. 1999; Dormal and Pesenti 2009; Eger et al. 2003; Piazza et al. 2007; Pinel et al. 2004) led to the postulation of a common magnitude representation (Hubbard et al. 2005; Walsh 2003). For example, Pinel et al. (2004) found that judging numerosity, size and brightness activated overlapping brain regions in the parietal and frontal lobe and that the amount of overlap predicted the size of the behavioral interference effects observed in their subjects. The authors argued for a 'distributed but overlapping' representation of different magnitudes at the neuronal level. Also Dormal and Pesenti (2009) found overlapping

activation when subjects made judgments about length or numerosity and suggested a 'common mechanism or representation for length and numerosity processing' (Dormal and Pesenti 2009, p 2473). However, some data contradict the hypothesis of a common magnitude system for different quantity domains and suggest independent and dissociable processing of different quantity dimensions (Cappelletti et al. 2009; Casasanto et al. 2010; Castelli et al. 2006). Thus, whether or not the representation of different quantity types are represented by the same neural circuits is still debated.

Our current data suggest a more neuron-specific representation of magnitude types within the PFC. In agreement with our finding of 26 % of sample-selective PFC neurons, Tudusciuc and Nieder (2009) found a similar proportion of PFC neurons (31 %) encoding numerosity and line length quantity information during a delayed match-to-sample task. However, while Tudusciuc and Nieder (2009) also found a small proportion of neurons (20 % of selective neurons) tuned to both length and numerosity-selective cells, we did not find significantly overlapping magnitude-tuned neuron populations in PFC. We speculate that this discrepancy could be due to the higher task demands in the rule-based magnitude comparison paradigm we used for the current study. Monkeys were not only required to match a given quantity, but they also had to use this information flexibly in a rule-switching task. This task complexity could also contribute to the different findings in the above-mentioned human functional imaging studies (Dehaene et al. 1999; Dormal and Pesenti 2009; Eger et al. 2003; Piazza et al. 2007; Pinel et al. 2004).

Magnitude categories

We compared the amount and coding properties of neurons representing the three different magnitude dimensions between the three frontal brain areas. We did not find any differences in the proportion of cells representing spatial frequency, line length or numerosity stimuli, neither for PFC neurons nor for the rarely occurring sample-selective cells in PMd and CMA. A similar proportion of neurons were encoding spatial frequency (37 %), line length (48 %) and numerosity (28 %) in PFC. Furthermore, there were no differences regarding the strength (selectivity-strength index and AUROC value), discriminability (selectivity-sharpness index) and latency between the three different magnitude types.

Our results suggest that all three magnitude types, be it sensory spatial frequency, continuous line length or abstract, discrete numerosity stimuli, are readily represented by PFC neurons. Recently, it has been shown that numerosity-selective neurons already exist in naïve, untrained animals (Viswanathan and Nieder 2013) and thus numerosity might be considered as a natural category that is spontaneously represented without the need for prior training, comparable to less abstract magnitude types. Interestingly, the authors found such 'untrained' number neurons both in the ventral intraparietal area (VIP) and in the PFC. This is in line with the proposed parietofrontal network (Nieder and Miller 2004), which suggests that quantity information is first extracted from purely visual features in parietal cortex (Nieder and Miller 2004; Nieder et al. 2002; Tudusciuc and Nieder 2007, 2009), and is then, through strong bidirectional neuronal connections between parietal and PFC regions (Badre and D'Esposito 2009; Chafee and Goldman-Rakic 2000; Petrides 2005; Petrides and Pandya 2007), transmitted to the PFC, where it is amplified and integrated with the current behavioral rule.

Even though our current study was not geared toward the details of the magnitude coding scheme, some of the neurons exhibited peaked tuning curves (e.g., Fig. 5b) characteristic of a 'labeled-line code' found for abstract magnitudes in both trained (Nieder 2013; Jacob and Nieder 2014; Ott et al. 2014 Viswanathan and Nieder 2015; Ditz and Nieder 2015) and naïve animals (Viswanathan and Nieder 2013), and humans (Jacob and Nieder 2009; Nieder and Dehaene 2009; Jacob et al. 2012). In contrast, many studies on perceptual decision-making find that neurons encode sensory quantities (such as vibrotactile frequency) as a linear function of firing rate (Hernandez et al. 2010), which suggests a summation code. Similar findings are reported for decisions based on reward value (Hernadi et al. 2015; Padoa-Schioppa and Assad 2006). The reasons for this discrepancy are still debated. We speculate that a categorical representation (as required in our studies) might favor a labeled-line code. In our studies, monkeys are required to encode the magnitudes as discrete, absolute values at a precise position on a magnitude continuum (i.e., exactly '3,' not smaller or larger). A summation code, however, might be adopted if magnitudes need to be encoded as continuous, relative values. It would be interesting to find out whether the manner in which neurons encode quantity information depended on the precise task at hand.

Integration of quantity information and abstract behavioral rules

Most of the time, the mere representation of magnitudes is not sufficient to generate complex goal-directed behavior. Magnitude information has to be integrated with rule information to select an appropriate behavioral action. Recently, we reported that mainly the PFC harbors rule-selective neurons when quantitative rules were applied to multiple magnitude types (Eiselt and Nieder 2013, 2014). A population of PFC neurons represented the rule always in conjunction with a specific magnitude type, representing each quantity rule (i.e., 'longer than,'

'more than,' 'shorter than,' 'fewer than') separately (Eiselt and Nieder 2013). However, one-third of the rule-coding neurons represented the overarching 'magnitude rule,' thus encoding the abstract principle 'greater than' and 'less than' irrespective of the underlying magnitude type. Only cells in PFC showed the ability to abstractly encode the magnitude rule this way, suggesting its unique role for abstract rule representation (Eiselt and Nieder 2014). Together with the current result, we suggest that the PFC, in comparison with PMd and CMA, is special in integrating separate and distinct magnitude information with abstract, 'overarching' quantity principles to form goal-directed responses. However, it is worth mentioning that Romo and colleagues (Hernandez et al. 2010) found significant encoding of vibrotactile frequency stimuli, a sensory quantity, in the dorsal premotor cortex. Future studies need to explore whether this might be related to the tested modalities (visual versus tactile) or the specific task design (rule-switching task versus comparison task). In general, it is thought that posterior frontal regions such as PMd and CMA might be more involved in the execution of concrete rules (Badre and D'Esposito 2009; di Pelligrino and Wise 1991; Hoshi and Tanji 2006; Kurata et al. 2000; Passingham 1988; Picard and Strick 2001; Schumacher et al. 2003; Turken and Swick 1999) but see (Wallis and Miller 2003; Muhammad et al. 2006) rather than abstract rule coding and quantity.

Since PFC is also reciprocally connected to PMd and CMA (Badre and D'Esposito 2009; Barbas 1988; Barbas and Pandya 1987, 1989; Bates and Goldman-Rakic 1993; Petrides 2005; Petrides and Pandya 2007; Tanji and Hoshi 2008), it might send the resulting action plan downstream to these areas, where they are relayed to primary motor areas for the final motor execution signal, without the need to forward both the underlying quantitative information about the magnitude types and the abstract rule that has to be applied.

In conclusion, our results highlight the importance of prefrontal cortex neurons in representing quantity information during a rule-guided magnitude comparison task. Among the tested areas, only the PFC represented sensory and mnemonic quantity information and as such seems to be the key area for integrating the underlying magnitude information and abstract quantitative rules. Our data demonstrate similarities between representations of sensory, spatial and numerical magnitude dimensions.

Acknowledgments Supported by the Bernstein Center for Computational Neuroscience, Tuebingen (BMBF; FKZ: 01GQ1002).

References

Asaad WF, Rainer G, Miller EK (2000) Task-specific neural activity in the primate prefrontal cortex. J Neurophysiol 84:451–459

Badre D, D'Esposito M (2009) Is the rostro-caudal axis of the frontal lobe hierarchical? Nat Rev Neurosci 10:659–669

Barbas H (1988) Anatomic organization of basoventral and mediodorsal visual recipient prefrontal regions in the rhesus monkey. J Comp Neurol 276:313–342

Barbas H, Pandya DN (1987) Architecture and frontal cortical connections of the premotor cortex (area 6) in the rhesus monkey. J Comp Neurol 256:211–288

Barbas H, Pandya DN (1989) Architecture and intrinsic connections of the prefrontal cortex in the rhesus monkey. J Comp Neurol 286:353–375

Bates JF, Goldman-Rakic PS (1993) Prefrontal connections of medial motor areas in the rhesus monkey. J Comp Neurol 336:211–288

Bongard S, Nieder A (2010) Basic mathematical rules are encoded by primate prefrontal cortex neurons. Proc Natl Acad Sci USA 107:2277–2282

Cappelletti M, Freeman ED, Cipolotti L (2009) Dissociations and interactions between time, numerosity and space processing. Neuropsychologia 47:2732–2748

Casasanto D, Fotakopoulou O, Boroditsky L (2010) Space and time in the child's mind: evidence for a cross-dimensional asymmetry. Cogn Sci 34:387–405

Castelli F, Glaser DE, Butterworth B (2006) Discrete and analogue quantity processing in the parietal lobe: a functional MRI study. Proc Natl Acad Sci USA 103:4693–4698

Chafee MV, Goldman-Rakic PS (2000) Inactivation of parietal and prefrontal cortex reveals interdependence of neural activity during memory-guided saccades. J Neurophysiol 83:1550–1566

Constantinidis C, Franowics MN, Goldman-Rakic PS (2001) The sensory nature of mnemonic representation in the primate prefrontal cortex. Nat Neurosci 4:311–316

de Hevia MD, Girelli L, Bricolo E, Vallar G (2008) The representational space of numerical magnitude: illusions of length. Q J Exp Psychol 61:1496–1514

De Valois RL, Albrecht DG, Thorell LG (1982) Spatial frequency selectivity of cells in macaque visual cortex. Vis Res 22:545–559

Dehaene S, Changeux JP (1993) Development of elementary numerical abilities: a neuronal model. J Cogn Neurosci 5:390–407

Dehaene S, Spelke E, Stanescu R, Pinel P, Tsivkin S (1999) Sources of mathematical thinking: behavioral and brain-imaging evidence. Science 284:970–974

di Pelligrino G, Wise SP (1991) A neurophysiological comparison of three distinct regions of the primate frontal lobe. Brain 114:951–978

Diester I, Nieder A (2008) Complementary contributions of prefrontal neuron classes in abstract numerical categorization. J Neurosci 28:7737–7747

Ditz HM, Nieder A (2015) Neurons selective to the number of visual items in the corvid songbird endbrain. Proc Natl Acad Sci USA 112:7827–7832

Dormal V, Pesenti M (2007) Numerosity-length interference: a Stroop experiment. Exp Psychol 54:289–297

Dormal V, Pesenti M (2009) Common and specific contributions of the intraparietal sulci to numerosity and length processing. Hum Brain Mapp 30:2466–2476

Eger E, Sterzer P, Russ MO, Giraud AL, Kleinschmidt A (2003) A supramodal number representation in human intraparietal cortex. Neuron 37:719–725

Eiselt AK, Nieder A (2013) Representation of abstract quantitative rules applied to spatial and numerical magnitudes in primate prefrontal cortex. J Neurosci 33:7526–7534

Eiselt AK, Nieder A (2014) Rule-activity related to spatial and numerical magnitudes: comparison of prefrontal, premotor and cingulate motor cortices. J Cogn Neurosci 26:1000–1012

Genovesio A, Brasted PJ, Mitz AR, Wise SP (2005) Prefrontal cortex activity related to abstract response strategies. Neuron 47:307–320

Genovesio A, Tsujimoto S, Wise SP (2009) Feature- and order-based timing representations in the frontal cortex. Neuron 63:254–266
Genovesio A, Tsujimoto S, Wise SP (2011) Prefrontal cortex activity during the discrimination of relative distance. J Neurosci 31:3968–3980
Green DM, Swets JA (1966) Signal detection theory and psychophysics. Wiley, New York
Hayashi MJ, Kanai R, Tanabe HC, Yoshida Y, Carlson S, Walsh V, Sadato N (2013) Interaction of numerosity and time in prefrontal and parietal cortex. J Neurosci 33:883–893
Henik A, Tzelgov H (1982) Is three greater than five: the relation between physical and semantic size in comparison tasks. Mem Cognit 10:389–395
Hernadi I, Grabenhorst F, Schultz W (2015) Planning activity for internally generated reward goals in monkey amygdala neurons. Nat Neurosci 18:461–469
Hernandez A, Nacher V, Luna R, Zainos A, Lemus L, Alvarez M, Vazquez Y, Camarillo L, Romo R (2010) Decoding a perceptual decision process across cortex. Neuron 66:300–314
Hoshi E, Tanji J (2006) Differential involvement of neurons in the dorsal and ventral premotor cortex during processing of visual signals for action planning. J Neurophysiol 95:3596–3616
Hoshi E, Shima K, Tanji J (1998) Task-dependent selectivity of movement-related neuronal activity in the primate prefrontal cortex. J Neurophysiol 80:3392–3397
Hubbard EM, Piazza M, Pinel P, Dehaene S (2005) Interactions between number and space in parietal cortex. Nat Rev Neurosci 6:435–448
Hussar CR, Pasternak T (2009) Flexibility of sensory representations in prefrontal cortex depends on cell type. Neuron 64:730–743
Hussar CR, Pasternak T (2012) Memory-guided sensory comparison in the prefrontal cortex: contribution of putative pyramidal cells and interneurons. J Neurosci 32:2747–2761
Hussar CR, Pasternak T (2013) Common rules guide comparison of speed and direction of motion in the dorsolateral prefrontal cortex. J Neurosci 33:972–986
Issa NP, Trepel C, Stryker MP (2000) Spatial frequency maps in cat visual cortex. J Neurosci 20:8504–8515
Jacob SN, Nieder A (2009) Tuning to non-symbolic proportions in the human frontoparietal cortex. Eur J Neurosci 30:1432–1442
Jacob SN, Nieder A (2014) Complementary roles for primate frontal and parietal cortex in guarding working memory from distractor stimuli. Neuron 83:226–237
Jacob SN, Vallentin D, Nieder A (2012) Relating magnitudes: the brain's code for proportions. Trends Cogn Sci 16:157–166
Kurata K, Tsuji T, Naraki S, Seino M, Abe Y (2000) Activation of the dorsal premotor cortex and pre-supplementary motor area of humans during an auditory conditional motor task. J Neurophysiol 84:1667–1672
Lu A, Hodges B, Zhang J, Zhang JX (2009) Contextual effects on number-time interaction. Cognition 113:117–122
Maffei L, Fiorentini A (1973) The visual cortex as a spatial frequency analyzer. Vis Res 13:1255–1267
Merten K, Nieder A (2012) Active encoding of decisions about stimulus absence in primate prefrontal cortex neurons. Proc Natl Acad Sci USA 109:6289–6294
Merten K, Nieder A (2013) Comparison of abstract decision encoding in the monkey prefrontal cortex, the presupplementary and cingulate motor areas. J Neurophysiol 110:19–32
Muhammad R, Wallis JD, Miller EK (2006) A comparison of abstract rules in the prefrontal cortex, premotor cortex, the inferior temporal cortex and the striatum. J Cogn Neurosci 18:974–989
Nieder A (2009) Prefrontal cortex and the evolution of symbolic reference. Curr Opin Neurobiol 19:99–108
Nieder A (2013) Coding of abstract quantity by 'number neurons' of the primate brain. J Comp Physiol A 199:1–16
Nieder A, Dehaene S (2009) Representation of number in the brain. Annu Rev Neurosci 32:185–208
Nieder A, Miller EK (2004) A parieto-frontal network for visual numerical information in the monkey. Proc Natl Acad Sci USA 101:7457–7462
Nieder A, Freedman DJ, Miller EK (2002) Representation of the quantity of visual items in the primate prefrontal cortex. Science 297:1708–1711
Onoe H, Komori M, Onoe K, Takechi H, Tsukada H, Watanabe Y (2001) Cortical networks recruited for time perception: a monkey positron emission tomography (PET) study. Neuroimage 13:37–45
Ott T, Jacob SN, Nieder A (2014) Dopamine receptors differentially enhance rule coding in primate prefrontal cortex neurons. Neuron 84:1317–1328
Padoa-Schioppa C, Assad JA (2006) Neurons in the orbitofrontal cortex encode economic value. Nature 441:223–226
Passingham RE (1988) Premotor cortex and preparation for movement. Exp Brain Res 70:590–596
Peng X, van Essen DC (2005) Peaked encoding of relative luminance in macaque areas V1 and V2. J Neurophysiol 93:1620–1632
Petrides M (2005) Lateral prefrontal cortex: architectonic and functional organization. Philos Trans R Soc Lond B Biol Sci 360:781–795
Petrides M, Pandya DN (2007) Efferent association pathways from the rostral prefrontal cortex in the macaque monkey. J Neurosci 27:11573–11586
Piazza M, Pinel P, Le Bihan D, Dehaene S (2007) A magnitude code common to numerosities and number symbols in human intraparietal cortex. Neuron 53:293–305
Picard N, Strick PL (2001) Imaging the premotor areas. Curr Opin Neurobiol 11:663–672
Pinel P, Piazza M, Le Bihan D, Dehaene S (2004) Distributed and overlapping cerebral representation of number, size, and luminance during comparative judgments. Neuron 41:1–20
Rao SM, Mayer AR, Harrington DL (2001) The evolution of brain activation during temporal processing. Nat Neurosci 4:317–323
Robson JG, Tolhurst DJ, Freeman RD, Ohzawa I (1988) Simple cells in the visual cortex of the cat can be narrowly tuned for spatial frequency. Vis Neurosci 1:415–419
Romo R, Brody CD, Hernandez A, Lemus L (1999) Neuronal correlates of parametric working memory in the prefrontal cortex. Nature 399:470–473
Schumacher EH, Elston PA, D'Esposito M (2003) Neural evidence for representation-specific response selection. J Cogn Neurosci 15:1111–1121
Schwarz W, Eiselt AK (2009) The perception of temporal order along the mental number line. J Exp Psychol Hum Percept Perform 35:989–1004
Tanji J, Hoshi E (2008) Role of lateral prefrontal cortex in executive behavioral control. Physiol Rev 88:37–57
Tudusciuc O, Nieder A (2007) Neuronal population coding of continuous and discrete quantity in the primate posterior parietal cortex. Proc Natl Acad Sci USA 104:14513–14518
Tudusciuc O, Nieder A (2009) Contributions of primate prefrontal and posterior parietal cortices to length and numerosity representation. J Neurophysiol 101:2984–2994
Turken AU, Swick D (1999) Response selection in the human anterior cingulate cortex. Nat Neurosci 2:920–924
Vallentin D, Nieder A (2008) Behavioral and prefrontal representation of spatial proportions in the monkey. Curr Biol 18:1420–1425
Vallentin D, Nieder A (2010) Representations of visual proportions in the primate posterior parietal and prefrontal cortices. Eur J Neurosci 32:1380–1387

Viswanathan P, Nieder A (2013) Neuronal correlates of a visual 'sense of number' in primate parietal and prefrontal cortices. Proc Natl Acad Sci USA 110:11187–11192

Viswanathan P, Nieder A (2015) Differential impact of behavioral relevance on quantity coding in primate frontal and parietal neurons. Curr Biol 25:1259–1269

Wallis JD, Miller EK (2003) From rule to response: neuronal processes in the premotor and prefrontal cortex. J Neurophysiol 90:1790–1806

Wallis JD, Anderson KC, Miller EK (2001) Single neurons in prefrontal cortex encode abstract rules. Nature 411:953–956

Walsh V (2003) A theory of magnitude: common cortical metrics of time, space and quantity. Trends Cogn Sci 7:483–488

White IM, Wise SP (1999) Rule-dependent neuronal activity in the prefrontal cortex. Exp Brain Res 126:315–335

Xuan B, Zhang D, He S, Chen X (2007) Larger stimuli are judged to last longer. J Vis 7(2):1–5